

AD

TECHNICAL REPORT ARCCB-TR-97012

**DESIGN AND VALIDATION OF A  
GUN BARREL VIBRATION ABSORBER**

ERIC L. KATHE

MAY 1997



**US ARMY ARMAMENT RESEARCH,  
DEVELOPMENT AND ENGINEERING CENTER  
CLOSE COMBAT ARMAMENTS CENTER  
BENÉT LABORATORIES  
WATERVLIET, N.Y. 12189-4050**



APPROVED FOR PUBLIC RELEASE; DISTRIBUTION UNLIMITED

19970606 150

## **DISCLAIMER**

The findings in this report are not to be construed as an official Department of the Army position unless so designated by other authorized documents.

The use of trade name(s) and/or manufacturer(s) does not constitute an official indorsement or approval.

## **DESTRUCTION NOTICE**

For classified documents, follow the procedures in DoD 5200.22-M, Industrial Security Manual, Section II-19 or DoD 5200.1-R, Information Security Program Regulation, Chapter IX.

For unclassified, limited documents, destroy by any method that will prevent disclosure of contents or reconstruction of the document.

For unclassified, unlimited documents, destroy when the report is no longer needed. Do not return it to the originator.

# REPORT DOCUMENTATION PAGE

*Form Approved  
OMB No. 0704-0188*

Public reporting burden for this collection of information is estimated to average 1 hour per response, including the time for reviewing instructions, searching existing data sources, gathering and maintaining the data needed, and completing and reviewing the collection of information. Send comments regarding this burden estimate or any other aspect of this collection of information, including suggestions for reducing this burden, to Washington Headquarters Services, Directorate for Information Operations and Reports, 1215 Jefferson Davis Highway, Suite 1204, Arlington, VA 22202-4302, and to the Office of Management and Budget, Paperwork Reduction Project (0704-0188), Washington, DC 20503.

<b>1. AGENCY USE ONLY (Leave blank)</b>	<b>2. REPORT DATE</b>	<b>3. REPORT TYPE AND DATES COVERED</b>
May 1997	Final	
<b>4. TITLE AND SUBTITLE</b> <b>DESIGN AND VALIDATION OF A GUN BARREL VIBRATION ABSORBER</b>		<b>5. FUNDING NUMBERS</b> AMCMS No. 6226.24.H180.0 PRON No. 4A6C6FYA1ABJ
<b>6. AUTHOR(S)</b>  Eric L. Kathe		
<b>7. PERFORMING ORGANIZATION NAME(S) AND ADDRESS(ES)</b>  U.S. Army ARDEC Benet Laboratories, AMSTA-AR-CCB-O Watervliet, NY 12189-4050		<b>8. PERFORMING ORGANIZATION REPORT NUMBER</b>  ARCCB-TR-97012
<b>9. SPONSORING/MONITORING AGENCY NAME(S) AND ADDRESS(ES)</b>  U.S. Army ARDEC Close Combat Armaments Center Picatinny Arsenal, NJ 07806-5000		<b>10. SPONSORING/MONITORING AGENCY REPORT NUMBER</b>
<b>11. SUPPLEMENTARY NOTES</b> Presented at the 67th Shock and Vibration Symposium, Monterey, CA, 18-22 November 1996. Published in proceedings of the symposium.		
<b>12a. DISTRIBUTION / AVAILABILITY STATEMENT</b>  Approved for public release; distribution unlimited.		<b>12b. DISTRIBUTION CODE</b>
<b>13. ABSTRACT (Maximum 200 words)</b>  This paper presents an applied method for the optimal design of passive vibration absorbers to reduce terrain-induced vibrations of tank cannons. The method uses a finite element model of the cannon. The design is optimized by assigning a scalar cost function to the frequency response of the modified barrel. The results indicate that the peak amplitude of the frequency response of a 1,500 Kg barrel may be cut in half by an appropriately tuned 20 Kg absorber. Experimental validation of the results using modal impact testing are shown.		
<b>14. SUBJECT TERMS</b>  Vibration Absorbers, Passive, Design, Cannons, Gun Barrels, Finite Element Method		<b>15. NUMBER OF PAGES</b> 15
<b>16. PRICE CODE</b>		
<b>17. SECURITY CLASSIFICATION OF REPORT</b> UNCLASSIFIED	<b>18. SECURITY CLASSIFICATION OF THIS PAGE</b> UNCLASSIFIED	<b>19. SECURITY CLASSIFICATION OF ABSTRACT</b> UNCLASSIFIED
		<b>20. LIMITATION OF ABSTRACT</b> UL

## GENERAL INSTRUCTIONS FOR COMPLETING SF 298

The Report Documentation Page (RDP) is used in announcing and cataloging reports. It is important that this information be consistent with the rest of the report, particularly the cover and title page. Instructions for filling in each block of the form follow. It is important to stay *within the lines* to meet optical scanning requirements.

**Block 1. Agency Use Only (Leave blank).**

**Block 2. Report Date.** Full publication date including day, month, and year, if available (e.g. 1 Jan 88). Must cite at least the year.

**Block 3. Type of Report and Dates Covered.**

State whether report is interim, final, etc. If applicable, enter inclusive report dates (e.g. 10 Jun 87 - 30 Jun 88).

**Block 4. Title and Subtitle.** A title is taken from the part of the report that provides the most meaningful and complete information. When a report is prepared in more than one volume, repeat the primary title, add volume number, and include subtitle for the specific volume. On classified documents enter the title classification in parentheses.

**Block 5. Funding Numbers.** To include contract and grant numbers; may include program element number(s), project number(s), task number(s), and work unit number(s). Use the following labels:

C - Contract	PR - Project
G - Grant	TA - Task
PE - Program Element	WU - Work Unit Accession No.

**Block 6. Author(s).** Name(s) of person(s) responsible for writing the report, performing the research, or credited with the content of the report. If editor or compiler, this should follow the name(s).

**Block 7. Performing Organization Name(s) and Address(es).** Self-explanatory.

**Block 8. Performing Organization Report Number.** Enter the unique alphanumeric report number(s) assigned by the organization performing the report.

**Block 9. Sponsoring/Monitoring Agency Name(s) and Address(es).** Self-explanatory.

**Block 10. Sponsoring/Monitoring Agency Report Number. (If known)**

**Block 11. Supplementary Notes.** Enter information not included elsewhere such as: Prepared in cooperation with...; Trans. of...; To be published in.... When a report is revised, include a statement whether the new report supersedes or supplements the older report.

**Block 12a. Distribution/Availability Statement.**

Denotes public availability or limitations. Cite any availability to the public. Enter additional limitations or special markings in all capitals (e.g. NOFORN, REL, ITAR).

**DOD** - See DoDD 5230.24, "Distribution Statements on Technical Documents."

**DOE** - See authorities.

**NASA** - See Handbook NHB 2200.2.

**NTIS** - Leave blank.

**Block 12b. Distribution Code.**

**DOD** - Leave blank.

**DOE** - Enter DOE distribution categories from the Standard Distribution for Unclassified Scientific and Technical Reports.

**NASA** - Leave blank.

**NTIS** - Leave blank.

**Block 13. Abstract.** Include a brief (*Maximum 200 words*) factual summary of the most significant information contained in the report.

**Block 14. Subject Terms.** Keywords or phrases identifying major subjects in the report.

**Block 15. Number of Pages.** Enter the total number of pages.

**Block 16. Price Code.** Enter appropriate price code (**NTIS only**).

**Blocks 17. - 19. Security Classifications.** Self-explanatory. Enter U.S. Security Classification in accordance with U.S. Security Regulations (i.e., UNCLASSIFIED). If form contains classified information, stamp classification on the top and bottom of the page.

**Block 20. Limitation of Abstract.** This block must be completed to assign a limitation to the abstract. Enter either UL (unlimited) or SAR (same as report). An entry in this block is necessary if the abstract is to be limited. If blank, the abstract is assumed to be unlimited.

## TABLE OF CONTENTS

<b>INTRODUCTION .....</b>	<b>1</b>
<b>THE DYNAMIC MODEL .....</b>	<b>2</b>
The Barrel .....	2
Constraint/Mounting of the Barrel .....	3
Damping .....	3
Coupled External Vibration Absorbers .....	4
Equation of Motion .....	5
Conversion to Single-Input/Single-Output First-Order State-Space .....	5
Bode Analysis .....	5
<b>FREQUENCY DOMAIN OPTIMIZATION OF THE ABSORBER .....</b>	<b>6</b>
Bode Analysis for Absorber Optimization .....	6
Optimization Surface .....	7
<b>EXPERIMENTAL VALIDATION .....</b>	<b>8</b>
Experimental Frequency Response Functions .....	8
Simulation of Tested Absorber Configurations .....	10
<b>CONCLUSION .....</b>	<b>12</b>
<b>REFERENCES .....</b>	<b>13</b>

### List of Tables

1. Measured frequencies, critical damping ratios, and the calculated Rayleigh damping coefficients .....
2. Measured parameters of the two 18.4Kg absorbers tested .....

### List of Figures

1. XM291 tank gun geometry and node locations used for finite element formulation ...
2. Grounded mounting of gun system .....
3. Population of absorber modified system matrices .....

4.	Juxtaposition of modified and unmodified barrels and the resulting relative frequency response .....	6
5.	Weighting function used to emphasize expected disturbance frequency content in the optimization .....	6
6.	Optimization surface in the design parameter space of an 18Kg absorber .....	8
7.	Simulated frequency response function of optimal absorbers of Figure 6 .....	9
8.	Simulated relative frequency response, $G_R(f)$ , of optimal absorber configurations ....	9
9.	Experimental frequency response function of unmodified gun system and two absorber configurations .....	10
10.	Experimental relative frequency response, $G_R(f)$ , of tested absorber configurations ..	11
11.	Simulated frequency response function of tested absorber configurations .....	11
12.	Simulated relative frequency response, $G_R(f)$ , of tested absorber configurations ....	12

## INTRODUCTION

This paper presents an applied method for the optimal design of passive vibration absorbers to reduce terrain-induced vibrations of tank cannons. It is anticipated that this will improve the accuracy of the weapon by reducing variations in the initial conditions of the gun barrel at the commencement of firing dynamics. The paper focuses on the attenuation of vibration in the vertical plane; application to the horizontal modes follows in analogy.

Flexural vibration of large caliber gun barrels has become more of an issue due to the increased exit velocity and fire-on-the-move demands placed on the weapon system to defeat reactive armor-protected threats at extended ranges. The velocity requirement results in longer barrels that have lower fundamental modes of vibrations and that are susceptible to flexural vibration both before and during firing dynamics. Reducing the flexural state of the barrel caused by terrain-induced vibrations—exclusive of the firing event—via a passive absorber enhances the overall performance of the weapon. Controlling vibrations during the firing cycle is more challenging because of the speed of the process; it is too fast for an absorber to shift or dissipate significant energy. Thus, the goal is to reduce the problem before shot-start.

Applying vibration absorbers to beams entails coupling a damped mass-spring system to the beam at the location of greatest vibration activity. This achieves two main benefits. First, the addition of the absorber reshapes the receptance of the system by shifting the resonant modes and zeros. Reshaping the frequency response away from known disturbance frequency bands effectively *rejects* the disturbance energy. Second, the absorber enhances the dissipation of vibrational energy. This second benefit is commonly misunderstood to always be the dominant mechanism by which the absorber reduces vibrations.

Actively controlling structural vibrations via an improved elevation servo-stabilization system is currently being investigated by the Advanced Drives and Weapon Stabalization Laboratory, ARDEC, AMSTA-AR-FSF-R. However, this approach is complicated by the non-minimum phase (right-hand-plane zeros) behavior of the essentially cantilevered beam system and limitations of the current hardware, which may require a significant upgrade for successful implementation. Incorporating a passive absorber does not preclude integration with active control techniques and may even enhance them.

The method presented in this paper uses a Euler-Bernoulli finite element technique to generate the second-order equations of motion of the gun barrel as a non-uniform beam, with subsequent conversion to the first-order state-space domain.<sup>[1]</sup> This model is then transformed to the frequency domain using the MATLAB® software package.<sup>[2,3]</sup> The design is optimized by assigning a scalar cost function to the frequency response function of the modified barrel; this provides a metric for minimization in the design parameter space of the vibration absorber. This applied approach forms a middle ground between mere numerical simulation and analytic formulation of the problem.

## THE DYNAMIC MODEL

### The Barrel

The finite element method was chosen to dynamically model the barrel. This application uses the Euler-Bernoulli beam approximation and Hermite-cubic interpolation functions to form the inertial and stiffness matrices of the undamped second-order equations of motion<sup>[1,4]</sup> by approximating the continuous non-uniform beam as a finite number of discrete elements. Within each element, the interpolation functions are used to approximate the interior deformation. At the boundary between two elements (called a node), continuity of lateral displacement and slope are imposed. When assembled, the resulting finite element model dynamics—governed solely by the nodal displacements and rotations—closely approximate the dynamics of the non-uniform beam.

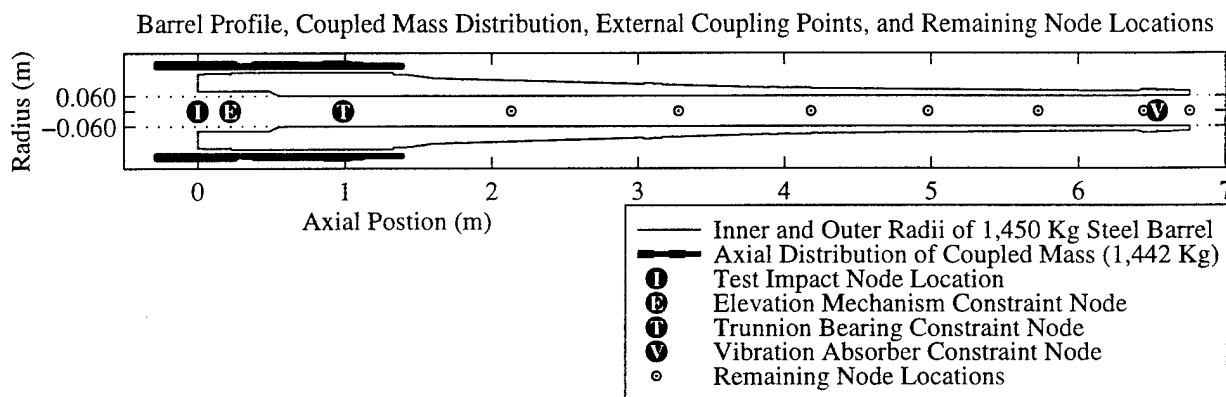


**Figure 1. XM291 tank gun geometry and node locations used for finite element formulation**

The XM291 geometry is shown in Figure 1. The plot depicts the inner and outer radii of the barrel with respect to axial position. The distribution of the coupled mass of components (such as the breech, cradle, and recuperators) attached to the barrel is represented by the thickness of the coaxial lines to the rear of the barrel. This mass increases the effective linear density of the beam. (Components (such as the breech) whose center of mass lies beyond the beam geometry are explicitly coupled to the end-node of the model after finite element formulation.) Impact testing, mount-constraint, and vibration absorber locations are also indicated. The muzzle-end sensor location lies to the immediate left of the absorber. Nodes are explicitly placed at these five points to facilitate external coupling with a 10 element model of the barrel. Of the remaining six nodes, one must be placed at the muzzle-end of the beam, which leaves five to be evenly placed by a meshing metric.<sup>[1]</sup> Mount constraints are later applied to eliminate the rigid body modes of the barrel and to emulate the boundary conditions of the barrel as tested. Finite element modeling of the barrel results in the unconstrained  $22 \times 22$  inertial (**M**) and cross-sectional stiffness (**K**) matrices that govern the  $22 \times 1$  generalized coordinate (**q**) and force (**f**) vectors. The generalized coordinate and force vector elements correspond to the alternating lateral and rotational states of the 11 nodes. Later on, these matrices and vectors will be modified and incorporated into the equation of motion, equation (2).

## Constraint/Mounting of the Barrel

Once the dynamics of the distributed parameter system of the barrel are modeled, they must be constrained by an approximation of the gun mount support. This constraint is applied to the barrel at two locations—the elevation mechanism and the trunnions. For this paper, the test structure was grounded by affixing a gun mount support to a pair of I-beams, which were bolted and epoxied to a concrete floor as depicted in Figure 2. The gun mount support directly constrains the trunnion bearing; a steel shaft (not visible) is pinned between the elevation mechanism attachment point and the gun mount support behind the trunnions.

Both constraint forces are modeled as stiff springs. For this analysis, both constraints were tuned (using a gradient descent method—the MATLAB® `<fmins>` command<sup>[2]</sup>) to match the first two experimental modal frequencies of the gun system. The equivalent spring at the elevation mechanism was set to  $65 \times 10^8$  N/m, and the trunnion rate was set to  $214 \times 10^8$  N/m. This altered the previous frequency values<sup>[5]</sup> by less than 10% and is consistent with the stiffer effective mounting of the trunnions relative to the elevation mechanism. Using arguments developed in Reference [1], the constraint stiffnesses are added to the diagonal elements of the finite element stiffness matrix that correspond to the lateral generalized coordinates of the constrained nodes,  $\mathbf{K}_{3,3}$  and  $\mathbf{K}_{5,5}$ , respectively.

This parametric formulation of the constraints is limited; the real structure would require more than two values for an accurate model. This approximation results in imprecise boundary conditions on the barrel. However, the model does capture many of the dynamic effects of interest and can easily be modified to incorporate more advanced constraint approximations—including servo-control dynamics.<sup>[6]</sup> In addition, tuning the boundary conditions to match the lowest two experimental modes of the system better characterizes the vibrations in the frequency regime of greatest interest.

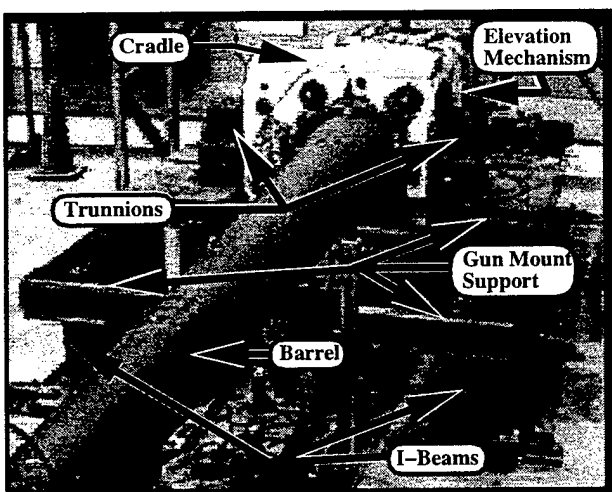


Figure 2. Grounded mounting of gun system

## Damping

A damping matrix ( $\mathbf{C}_D$ )—see equation (2)—that introduces a force opposite in direction and proportional to the velocity of the deformation is constructed by the Rayleigh proportional damping approximation ( $\mathbf{C}_D = \alpha\mathbf{M} + \beta\mathbf{K}$ ).<sup>[1,7,8]</sup> The critical damping ratios for the first two modes of the gun system were computed using the half-power method<sup>[8]</sup> on the measured frequency response (see Figure 9). The proportional damping coefficients were then assigned using equation (1).<sup>[1,7]</sup> The results are shown in Table 1. The temporal units of the damping coefficients are equivalent to damping (force/velocity) versus mass and damping versus stiffness, respectively.

**Table 1. Measured frequencies, critical damping ratios, and the calculated Rayleigh damping coefficients**

$\omega_1 = 7.25 \times 2\pi \text{ rad/sec}$	$\zeta_1 = 18\%$	$\alpha = 2.57 \text{ s}^{-1}$
$\omega_2 = 25.4 \times 2\pi \text{ rad/sec}$	$\zeta_2 = 5\%$	$\beta = 69.5 \times 10^{-6} \text{ s}$

$$\begin{bmatrix} \alpha \\ \beta \end{bmatrix} = 2 \begin{bmatrix} 1 & \omega_1^2 \\ 1 & \omega_2^2 \end{bmatrix}^{-1} \begin{bmatrix} \omega_1 \zeta_1 \\ \omega_2 \zeta_2 \end{bmatrix} \quad (1)$$

### Coupled External Vibration Absorbers

With the inclusion of the absorber, a new *energy-storing* degree of freedom is added to the total system. This requires a new generalized coordinate,  $q_{23}$ , to represent the deflection of the absorber and its time derivatives from its equilibrium position.<sup>[1]</sup> This requirement increases the size of the system matrices (to be used in equation (2)) from  $22 \times 22$  to  $23 \times 23$ .

Figure 3 depicts the population of the completed system mass and stiffness matrices of an absorber modified system. (The damping matrix formulation is analogous to the stiffness matrix.) The plots verify the cascading construction of  $4 \times 4$  elemental matrices—resulting in the diagonally banded system matrices for the  $22 \times 22$  finite element portion. Furthermore, coupling the absorber with parameters  $M_{VA}$ ,  $C_{VA}$ , and  $K_{VA}$  to the lateral generalized coordinate,  $q_{19}$ , increases  $K_{19,19}$  by  $K_{VA}$ ; places  $K_{VA}$  into  $K_{23,23}$ ; inserts  $-K_{VA}$  into  $K_{19,23}$  and  $K_{23,19}$ ; and places  $M_{VA}$  at  $M_{23,23}$ .

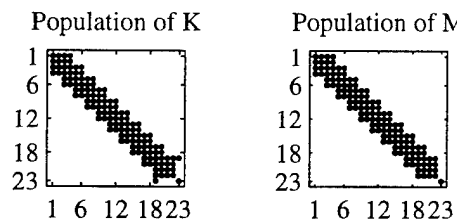


**Figure 3. Population of absorber modified system matrices**

## Equation of Motion

Once the combined system matrices are formed, the resulting equation of motion is as follows:

$$\mathbf{M}\ddot{\mathbf{q}} + \mathbf{C}_D\dot{\mathbf{q}} + \mathbf{K}\mathbf{q} = \mathbf{f} \quad (2)$$

where:

- |                |   |              |   |
|----------------|---|--------------|---|
| $\mathbf{M}$   | is the $23 \times 23$ mass matrix.      | $\mathbf{q}$ | is the $23 \times 1$ generalized coordinate vector. |
| $\mathbf{C}_D$ | is the $23 \times 23$ damping matrix.   | $\mathbf{f}$ | is the $23 \times 1$ generalized force vector.      |
| $\mathbf{K}$   | is the $23 \times 23$ stiffness matrix. | •            | denotes $d/dt$ .                                    |

## Conversion to Single-Input/Single-Output First-Order State-Space

The second-order symmetric equations of motion of equation (2) are transformed to first-order state-space using the method presented in References [1] and [4]. The multi-input/multi-output state-space model is then truncated to a single-input/single-output system for frequency response analysis. The input,  $f_1$ , is located at the node at the rear of the barrel where the modal hammer impacts are to be applied (see Figure 1). The measured deflection at the node before the absorber,  $q_{17}$ , is selected as the sole output of the system.

## Bode Analysis

Once in the single-input/single-output state-space realization, the frequency response of the system may be computed using the MATLAB® `bode` command.<sup>[3]</sup> The frequency response of a dynamic system indicates the steady-state response,  $y(t)$ , of the system to a sinusoidal input,  $u(t)$ <sup>[3]</sup> as

$$\begin{aligned} u(t) &= A \sin((2\pi f)t) \\ y(t) &= k A \sin((2\pi f)t + \phi) \end{aligned} \quad (3)$$

where:

- $u(t)$  is vertical input at the breech,  $f_1$  (N).
- $y(t)$  is response of the muzzle,  $q_{17}$  (m).
- $A$  is amplitude of the input force (N).
- $k$  is the receptance gain (m/N).
- $f$  is frequency of the input force (Hz).
- $\phi$  is phase of the response (rad).
- $t$  is time (s).

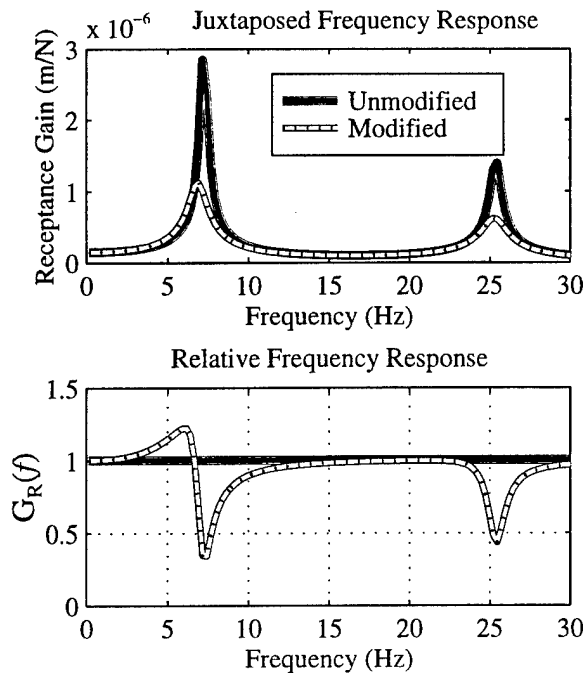


**Figure 4. Juxtaposition of modified and unmodified barrels and the resulting relative frequency response**

with a natural frequency,  $f_n$ , of nine Hz and a critical damping ratio,  $\zeta$ , of 40%. This was chosen to highlight a known but poorly characterized disturbance, which is introduced to the system through the tank suspension (a *low-pass filter*), and to reduce emphasis on the frequencies below the first mode of the system, which are adequately handled by the existing elevation servo-stabilization. In general, the weighting function combines the dynamics of the system with any a priori frequency characterization of the disturbance. (Multiplication in the frequency domain is equivalent to convolution in the time domain<sup>[9]</sup>). Thus, this weighting function approximates a *white* force spectrum that passed through a second-order, damped filter.

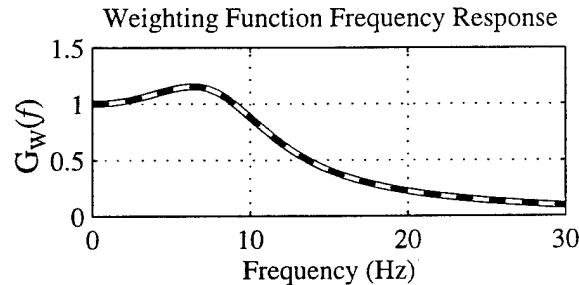


**Figure 5. Weighting function used to emphasize expected disturbance frequency content in the optimization**

## FREQUENCY DOMAIN OPTIMIZATION OF THE ABSORBER

### Bode Analysis for Absorber Optimization

The frequency response of the unmodified gun system is compared to the response when various parametric absorber configurations are coupled. For this paper, two absorber parameters are varied—the stiffness,  $K_{VA}$ , and the stiffness proportional damping coefficient,  $\beta_{VA}$ —while the mass,  $M_{VA}$ , is held constant at 18 Kg and the mass proportional coefficient,  $\alpha_{VA}$ , is set to zero. The gain function of the modified barrel is then divided by the gain of the original system—resulting in a relative frequency response,  $G_R(f)$ , as shown in Figure 4.

A weighting function,  $G_W(f)$ , is applied to emphasize known disturbances. This function, as shown in Figure 5, was generated as the normalized response of a second-order system

A single scalar cost function,  $J$ , is then quantitatively computed as the normalized integral of the weighted relative frequency response of the absorber modified system across its effective bandwidth

$$J = \frac{\int_{f_{low}}^{f_{high}} (G_R(f) G_W(f)) df}{\int_{f_{low}}^{f_{high}} G_W(f) df} \quad (4)$$

where:

$J$	is scalar cost function.	$f_{low}$	is lower bandwidth frequency.
$G_R(f)$	is relative frequency response.	$f_{high}$	is upper bandwidth frequency.
$G_W(f)$	is weighting function.		

Other cost functions could be used to incorporate other design considerations (such as worst-case performance) or pragmatic engineering issues (such as bounds on reasonable damping levels).

The flexibility provided by incorporating virtually any weighting function (including servo-control characterization and the potential for multi-mode receptance reduction) motivated the development of this technique. Analytical techniques for the optimal design of absorbers that are based on minimum-slope cross-over points<sup>[10, 11]</sup> or a quadratic cost function<sup>[12]</sup> were not used because they do not seamlessly integrate with this formulation.

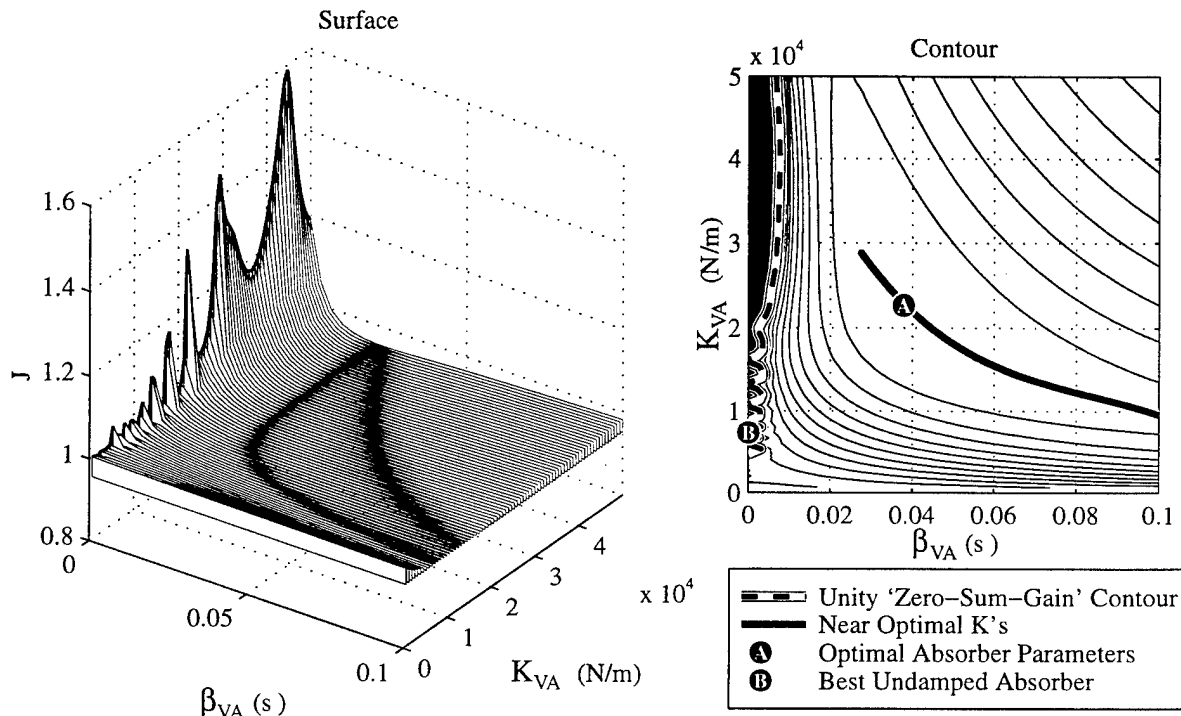
### Optimization Surface

Figure 6 shows the optimization surface generated for an 18 Kg vibration absorber across the bandwidth 0 to 16 Hz using the scalar frequency response cost function. The plots clearly indicate that for low levels of damping,  $\beta_{VA} < 0.01$  s, the absorber design is sensitive to parametric variation. This is seen by the high density of the contour lines near the peaks, which indicate step gradients. The peaks are caused by detrimental interaction of the absorber with the fundamental frequencies of the barrel and numerical integration errors for the undamped cases.

The contour plot indicates that the optimal undamped design—indicated by point **B** at  $K_{VA} = 7,333$  N/m—would effect disturbance rejection with a  $J$  value of 0.99. If decoupled from the barrel, it would have a natural frequency,  $f_n$ , of 3.18 Hz. For higher damping levels,  $0.02 \text{ s} < \beta_{VA}$ , the absorber design appears to be quite insensitive. The optimal absorber, indicated by point **A** at  $K_{VA} = 22,667$  N/m and  $\beta_{VA} = 37.9 \times 10^{-3}$  s, would effect disturbance rejection by the absorber with

a J value of 0.95. If decoupled from the barrel, it would have a damped natural frequency,  $f_d$ , of 4.17 Hz and a critical damping ratio,  $\zeta$ , of 67%.

The lack of sensitivity to design parameters for an optimal absorber is a desirable result. Engineering obstacles with damping materials that are subject to harsh variations in temperature—as would be experienced in a weapons environment—may be relaxed because of this lack of sensitivity.



**Figure 6. Optimization surface in the design parameter space of an 18Kg absorber**

Furthermore, the negative slope of the line of optimal  $K_{VA}$ 's with respect to  $\beta_{VA}$  is in-line with the temperature-dependent properties of visco-elastic polymers, one candidate technique for achieving the absorber damping.

The frequency response function and relative response of both of these optimal absorbers are shown in Figures 7 and 8, respectively. (A dB is related to the gain of equation (3) as  $20\log_{10}(k/k_o)$ , with the reference receptance,  $k_o$ , set to 1 m/N.)

## EXPERIMENTAL VALIDATION

### Experimental Frequency Response Functions

Two absorber configurations were experimentally evaluated and compared to the model. For pragmatic reasons, both absorbers were relatively low in damping compared to the optimal absorber design indicated in Figure 6 because proof of principle demonstration could be achieved with simple and available hardware.

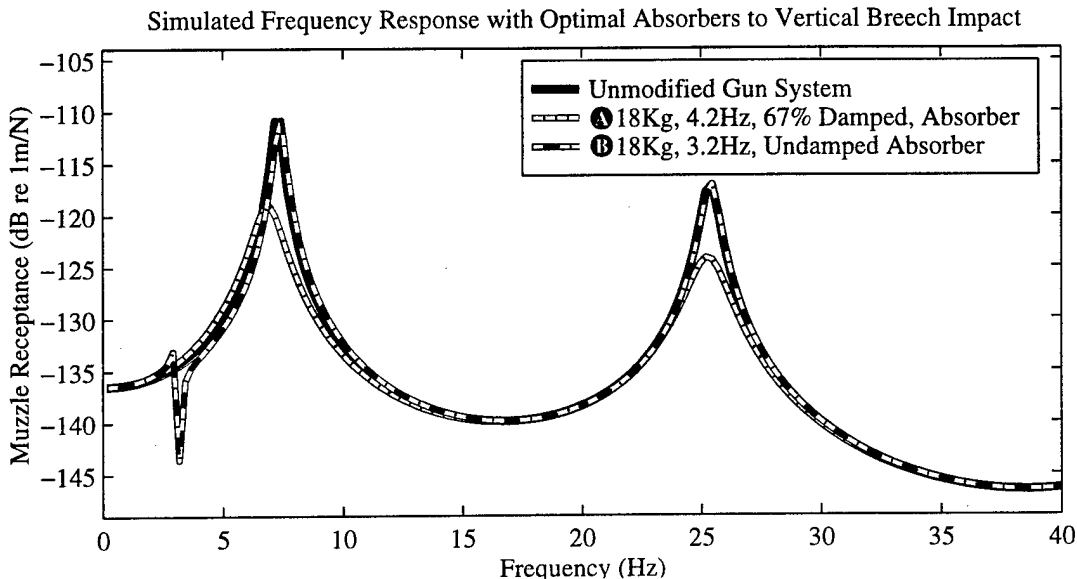


**Figure 7. Simulated frequency response function of optimal absorbers of Figure 6**

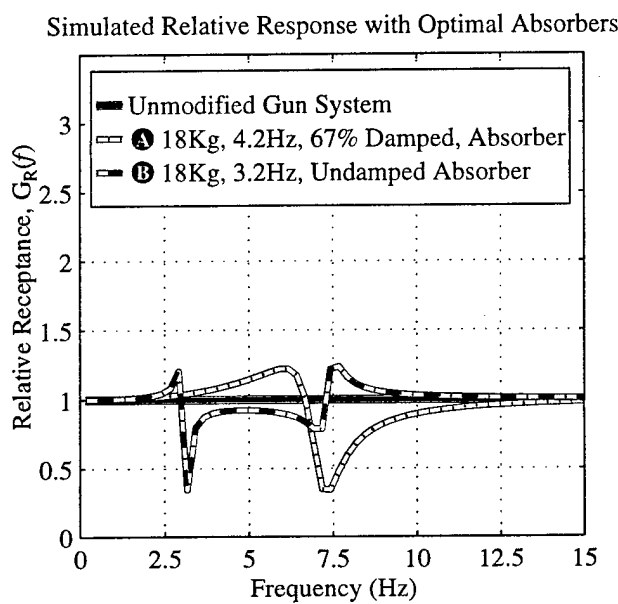


**Figure 8. Simulated relative frequency response,  $G_R(f)$ , of optimal absorber configurations**

The tests were conducted using a Hewlett-Packard 3566A spectrum analyzer, an instrumented 3-pound PCB modal impact hammer, and Electro-Mike PA12D  $\frac{1}{2}$ " eddy probe displacement sensors. Ten averages were used to smooth spurious variations in the measured frequency response function.<sup>[8]</sup>

The three frequency response functions measured are shown in Figure 9, with the relative response depicted in Figure 10. The absorber mass was set using calibrated weights. The remaining absorber parameters were inferred from the power spectrum and the transient decay of each absorber coupled to a rigid stand. The damped natural frequency,  $f_d$ , corresponds to the peak of the power spectrum. The damping was evaluated using the logarithmic decrement method.<sup>[8,10]</sup> The resulting absorber parameters are shown in Table 2.

**Table 2. Measured parameters of the two 18.4 Kg absorbers tested**

$K_{VA}$ (N/m)	$\beta_{VA}$ (s)	$f_d$ (Hz)	$\zeta$ (%)
11,900	0.000243	3.88	0.296
22,000	0.00230	5.50	3.97

Figure 9 clearly demonstrates that the first two modes dominate the response. Both vertical modes suffer some degree of cross-talk with the horizontal mode, which has a slightly higher frequency because of the rotational resistance of the opposed trunnions, which is not present in the vertical mode. The plot also reveals a lack of an asymptotic stiffness line<sup>[8]</sup> at the low frequencies and a discrepancy in the dB scale relative to that of the model. The cause of these two shortcomings is not certain and is believed to be a discrepancy in the analyzer configuration.

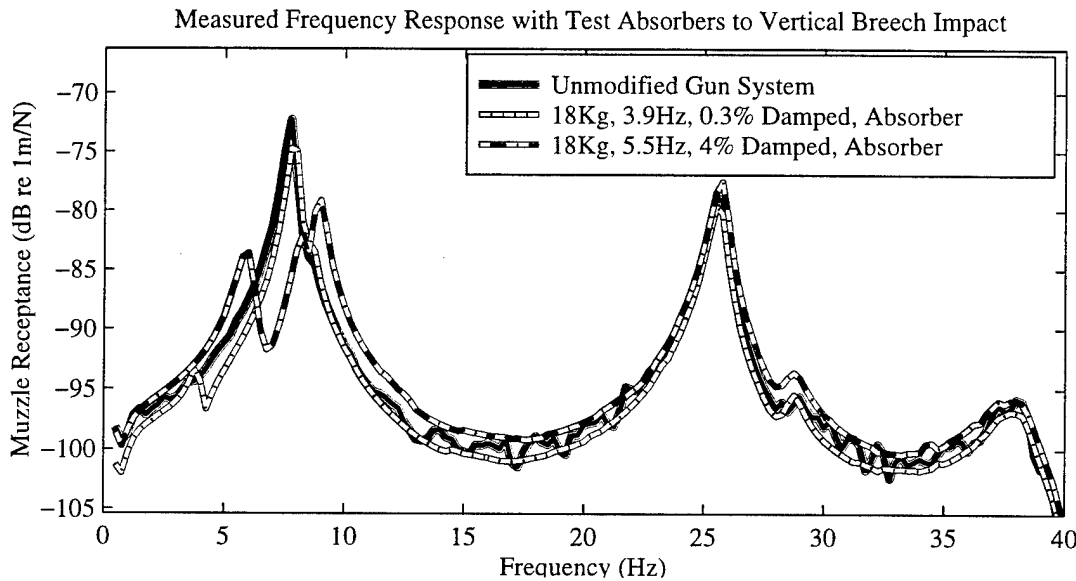


**Figure 9. Experimental frequency response function of unmodified gun system and two absorber configurations**

#### Simulation of Tested Absorber Configurations

Figures 11 and 12 depict the simulated frequency response of the three hardware configurations tested.

A comparison with Figures 9 and 10 indicates that the poles and zeros of the absorber were reasonably placed by the model. Discrepancies in the peak amplitudes of the absorber response are expected. Both absorbers are low in damping and rely heavily on the dissipation of the barrel to bound their response. These high peaks are “smoothed” by the finite frequency resolution of the

experimental results. The Bode analysis of the model is not subject to this; therefore, the peak response is sensitive to the specific frequencies evaluated in the vicinity of a pole or zero. It is important to note that the cost function,  $J$ , is sensitive to variation in these *narrow* peaks if the frequency vector used to numerically evaluate the integral of equation (4) is too coarse. The shift to higher frequency poles than were predicted for the stiffer absorber may be caused by the cross-talk between the vertical and horizontal modes of the test structure.

Measured Relative Response with Tested Absorbers

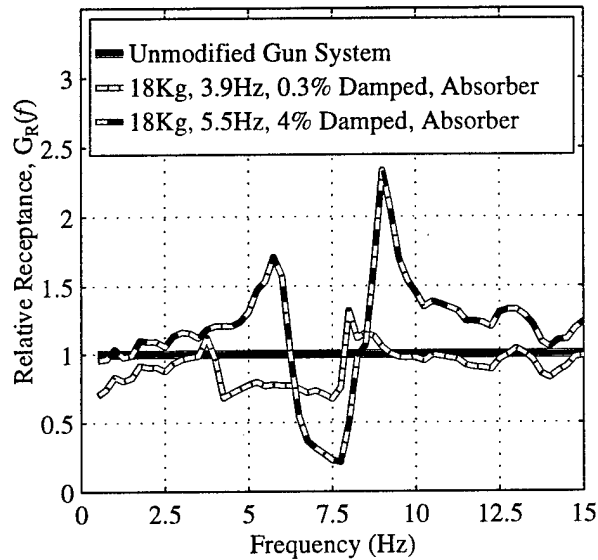


Figure 10. Experimental relative frequency response,  $G_R(f)$ , of tested absorber configurations

Simulated Frequency Response with Tested Absorbers to Vertical Breech Impact

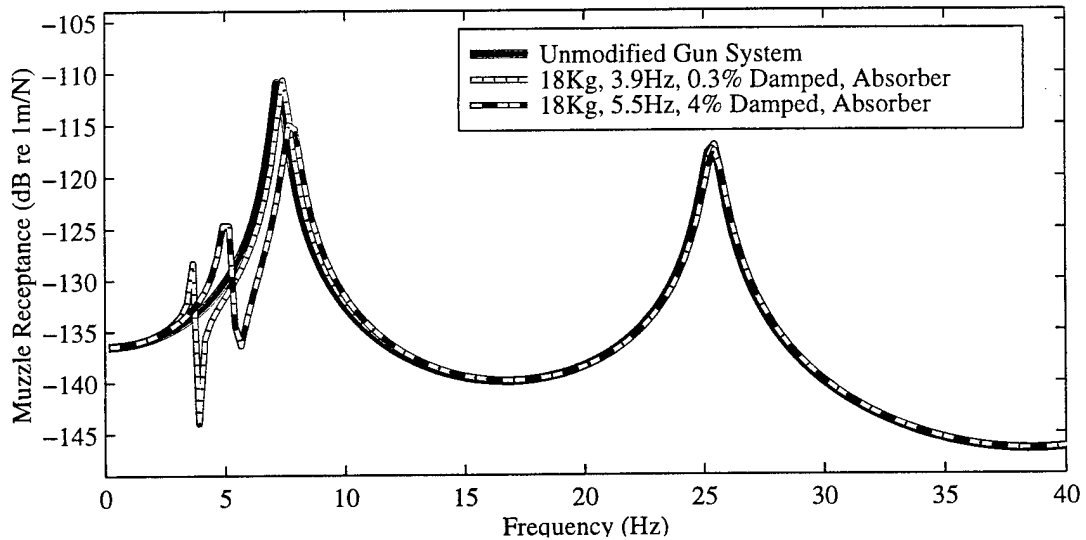


Figure 11. Simulated frequency response function of tested absorber configurations

## CONCLUSION

Applying a gun barrel vibration absorber to favorably reshape the frequency response of a tank cannon was shown. Significant reductions in amplitude—greater than 50%—were demonstrated, both experimentally and by the finite element model.

A general optimization procedure for designing an absorber that is insensitive to parametric uncertainty and that incorporates a priori disturbance characterization was presented.

The model of the coupled absorber/gun system was compared to experimental results. Tuning the unmodified barrel model to match the experimental fixture frequencies and damping ratios was implemented. This tuning does not artificially match the absorber effects; instead it provides a consistent baseline from which to evaluate the incorporation of the absorber into the model. Comparing the simulated and experimental frequency responses indicates that the modified system poles and zeros were properly placed by the model. Discrepancies in the narrow relative peaks of the absorber modified model response were explained by the smoothing effect inherent in the finite resolution experimental frequency response, which is not present in the Bode analysis of the model.

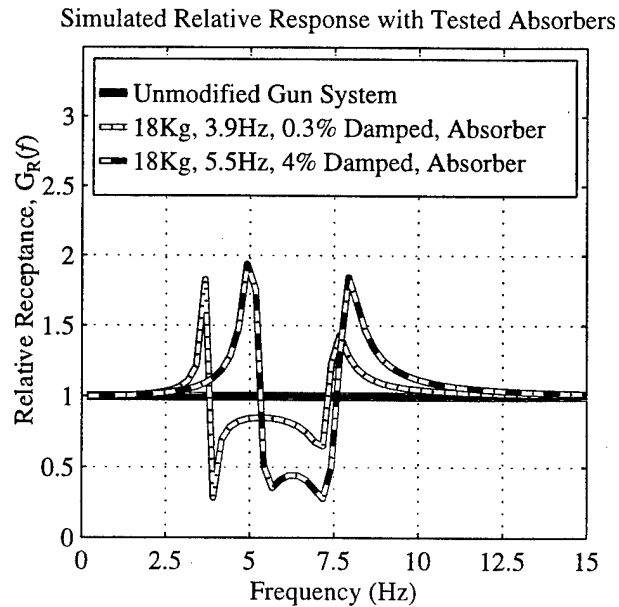


Figure 12. Simulated relative frequency response,  $G_R(f)$ , of tested absorber configurations

The graph illustrates the impact of different absorber configurations on the system's frequency response. The unmodified gun system (solid line) has a flat response. The 18Kg, 3.9Hz, 0.3% Damped, Absorber (dashed line) exhibits a sharp resonance peak at approximately 4.5 Hz and a corresponding anti-resonance dip at approximately 6.5 Hz. The 18Kg, 5.5Hz, 4% Damped, Absorber (dash-dot line) exhibits a broader resonance peak at approximately 5.5 Hz and a corresponding anti-resonance dip at approximately 7.5 Hz. These results are consistent with the experimental findings presented in the paper.

## REFERENCES

1. Kathe, E., "MATLAB® Modeling of Non-Uniform Beams Using the Finite Element Method for Dynamic Design and Analysis," U.S. Army ARDEC Report, ARCCB-TR-96010, Benet Laboratories, Watervliet, NY, April 1996.
2. *MATLAB® Reference Guide*, The MathWorks, Inc., Natick, MA, July 1993.
3. *Control System Toolbox User's Guide*, The MathWorks, Inc., Natick, MA, June 1994.
4. Meirovitch, L., *Dynamics and Control of Structures*, Wiley, NY, 1990.
5. Kathe, E., "Design of Passive Vibration Absorber to Reduce Terrain-Induced Gun Barrel Vibrations in the Frequency Domain," Proceedings of the Eighth U.S. Army Symposium on Gun Dynamics, ARCCB-SP-96032 Benet Laboratories, Watervliet, NY, May 14-16, 1996, pp 28-1 to 28-17.
6. Dholiwar, D. K., "Development of a Hybrid Distributed-Lumped Parameter Openloop Model of Elevation Axis for a Gun System," Proceedings of the Seventh U.S. Army Symposium on Gun Dynamics, ARCCB-SP-93034, Benet Laboratories, Watervliet, NY, 11-13 May 1993, pp. 368-385.
7. Kanchi, M. B., *Matrix Methods of Structural Analysis*, 2nd ed., Wiley, NY, 1993.
8. Ewins, D. J., *Modal Testing: Theory and Practice*, Wiley, NY, 1984.
9. Bracewell, R. N., *The Fourier Transform and Its Applications*, 2nd ed., McGraw-Hill, NY, 1986.
10. Dimarogonas, A., *Vibration for Engineers*, 2nd ed., Prentice Hall, Upper Saddle River, NJ, 1996.
11. Den Hartog, J., *Mechanical Vibrations*, 4th ed., McGraw-Hill, NY, 1956.
12. Juang, J. N., "Optimal Design of a Passive Vibration Absorber for a Truss Beam," AIAA Paper 83-2291, 1983.

---

TECHNICAL REPORT INTERNAL DISTRIBUTION LIST

	<u>NO. OF COPIES</u>
CHIEF, DEVELOPMENT ENGINEERING DIVISION ATTN: AMSTA-AR-CCB-DA	1
-DB	1
-DC	1
-DD	1
-DE	1
CHIEF, ENGINEERING DIVISION ATTN: AMSTA-AR-CCB-E	1
-EA	1
-EB	1
-EC	1
CHIEF, TECHNOLOGY DIVISION ATTN: AMSTA-AR-CCB-T	2
-TA	1
-TB	1
-TC	1
TECHNICAL LIBRARY ATTN: AMSTA-AR-CCB-O	5
TECHNICAL PUBLICATIONS & EDITING SECTION ATTN: AMSTA-AR-CCB-O	3
OPERATIONS DIRECTORATE ATTN: SIOWV-ODP-P	1
DIRECTOR, PROCUREMENT & CONTRACTING DIRECTORATE ATTN: SIOWV-PP	1
DIRECTOR, PRODUCT ASSURANCE & TEST DIRECTORATE ATTN: SIOWV-QA	1

---

NOTE: PLEASE NOTIFY DIRECTOR, BENÉT LABORATORIES, ATTN: AMSTA-AR-CCB-O OF ADDRESS CHANGES.

**TECHNICAL REPORT EXTERNAL DISTRIBUTION LIST**

<u>NO. OF COPIES</u>	<u>NO. OF COPIES</u>		
ASST SEC OF THE ARMY RESEARCH AND DEVELOPMENT ATTN: DEPT FOR SCI AND TECH THE PENTAGON WASHINGTON, D.C. 20310-0103	1	COMMANDER ROCK ISLAND ARSENAL ATTN: SMCRI-SEM ROCK ISLAND, IL 61299-5001	1
DEFENSE TECHNICAL INFO CENTER ATTN: DTIC-OCP (ACQUISITIONS) 8725 JOHN J. KINGMAN ROAD STE 0944 FT. BELVOIR, VA 22060-6218	2	COMMANDER U.S. ARMY TANK-AUTMV R&D COMMAND ATTN: AMSTA-DDL (TECH LIBRARY) WARREN, MI 48397-5000	1
COMMANDER U.S. ARMY ARDEC ATTN: AMSTA-AR-AEE, BLDG. 3022 AMSTA-AR-AES, BLDG. 321 AMSTA-AR-AET-O, BLDG. 183 AMSTA-AR-FSA, BLDG. 354 AMSTA-AR-FSM-E AMSTA-AR-FSS-D, BLDG. 94 AMSTA-AR-IMC, BLDG. 59 PICATINNY ARSENAL, NJ 07806-5000	1 1 1 1 1 1 2	COMMANDER U.S. MILITARY ACADEMY ATTN: DEPARTMENT OF MECHANICS WEST POINT, NY 10966-1792	1
DIRECTOR U.S. ARMY RESEARCH LABORATORY ATTN: AMSRL-DD-T, BLDG. 305 ABERDEEN PROVING GROUND, MD 21005-5066	1	U.S. ARMY MISSILE COMMAND REDSTONE SCIENTIFIC INFO CENTER ATTN: AMSMI-RD-CS-R/DOCUMENTS BLDG. 4484 REDSTONE ARSENAL, AL 35898-5241	2
DIRECTOR U.S. ARMY RESEARCH LABORATORY ATTN: AMSRL-WT-PD (DR. B. BURNS) ABERDEEN PROVING GROUND, MD 21005-5066	1	COMMANDER U.S. ARMY FOREIGN SCI & TECH CENTER ATTN: DRXST-SD 220 7TH STREET, N.E. CHARLOTTESVILLE, VA 22901	1
		COMMANDER U.S. ARMY LABCOM, ISA ATTN: SLCIS-IM-TL 2800 POWER MILL ROAD ADELPHI, MD 20783-1145	1

---

NOTE: PLEASE NOTIFY COMMANDER, ARMAMENT RESEARCH, DEVELOPMENT, AND ENGINEERING CENTER,  
BENÉT LABORATORIES, CCAC, U.S. ARMY TANK-AUTOMOTIVE AND ARMAMENTS COMMAND,  
AMSTA-AR-CCB-O, WATERVLIET, NY 12189-4050 OF ADDRESS CHANGES.

---

TECHNICAL REPORT EXTERNAL DISTRIBUTION LIST (CONT'D)

	<u>NO. OF COPIES</u>		<u>NO. OF COPIES</u>
COMMANDER U.S. ARMY RESEARCH OFFICE ATTN: CHIEF, IPO P.O. BOX 12211 RESEARCH TRIANGLE PARK, NC 27709-2211	1	WRIGHT LABORATORY ARMAMENT DIRECTORATE ATTN: WL/MNM EGLIN AFB, FL 32542-6810	1
DIRECTOR U.S. NAVAL RESEARCH LABORATORY ATTN: MATERIALS SCI & TECH DIV WASHINGTON, D.C. 20375	1	WRIGHT LABORATORY ARMAMENT DIRECTORATE ATTN: WL/MNMF EGLIN AFB, FL 32542-6810	1

NOTE: PLEASE NOTIFY COMMANDER, ARMAMENT RESEARCH, DEVELOPMENT, AND ENGINEERING CENTER,  
BENÉT LABORATORIES, CCAC, U.S. ARMY TANK-AUTOMOTIVE AND ARMAMENTS COMMAND,  
AMSTA-AR-CCB-O, WATERVLIET, NY 12189-4050 OF ADDRESS CHANGES.

---